BJRS
BRAZILIAN JOURNAL OF RADIATION SCIENCES

doi.org/10.15392/2319-0612.2024.2528
2024, 12(4A) | 01-17 | e2528
Submitted: 2024-06-25
Accepted: 2025-05-19

Manufacturing of Physical Phantom and Evaluation of a Software for Automated and Remote Quality Control in Mammography Using a Retrofit DR System

Almeida [a*], L. F. M.; Engler [a], C.; Squair [a], P. L.; Nogueira [a], M. S.

[a] Centro de Desenvolvimento da Tecnologia Nuclear, 31270-901, Belo Horizonte-MG, Brazil.

*Correspondence: lailafernanda8852@gmail.com

Abstract: Mammography is crucial for the early detection of breast cancer, requiring periodic quality controls to ensure that images and patient exposure doses comply with regulatory limits. This study addresses the challenges involved in conducting quality control, such as the lack of qualified personnel and the subjectivity of daily evaluations with phantoms. Additionally, the research proposes the incorporation of automated and remote quality control tools. In this context, a simple phantom was developed by the IAEA using materials such as copper, acrylic, and aluminum, to be used with the Automated Tool for Image Analysis (ATIA) software. This software performs automatic image analyses, extracting data from the DICOM header and exporting it to a CSV file for analysis in Excel® spreadsheets. The objectives of this work were: (a) to manufacture the phantom according to the standard model from the IAEA Human Health Series No. 39 publication; (b) to apply the ATIA software in the daily monitoring of a mammography unit and the digital radiography (DR) image receptor retrofitted to an analog mammography unit at the Laboratory of Radioprotection Applied to Mammography (LARAM) of CDTN; (c) to evaluate and compare the responses obtained between the automated ATIA software and the manual IMAGEJ software. The results demonstrated the stability and consistency of the mammography system in metrics such as SDNR and SNR, essential for ensuring image quality. However, variabilities in horizontal and vertical MTF at lower spatial frequencies indicate discrepancies in resolving fine details. The detectability index (D') stood out for its high consistency, indicating the reliability of the mammography system in detecting small details. Thus, it can be inferred that significant differences between quality control software in various metrics highlight the importance of careful software selection to meet specific mammographic evaluation needs.

Keywords: Mammography, Quality Control, Automation.

BJRS
BRAZILIAN JOURNAL OF RADIATION SCIENCES

doi.org/10.15392/2319-0612.2024.2528
2024, 12(4A) | 01-17 | e2528
Submitted: 2024-06-25
Accepted: 2025-05-19

Fabricação de Fantoma Físico e Avaliação de um Software para Controle de Qualidade Automatizado e Remoto em Mamografia Usando um Sistema Retrofit DR

Resumo: A mamografia é crucial para a detecção precoce do câncer de mama, exigindo controle de qualidade periódico para garantir que as imagens e as doses de exposição aos pacientes estejam dentro dos limites regulamentares. Dessa forma, este estudo aborda as problemáticas envolvidas que dificultam a realização de um controle de qualidade, como a falta de pessoal qualificado e a subjetividade das avaliações diárias com fantomas, além disso, a pesquisa propõe a incorporação de ferramentas automatizadas e remotas para controle de qualidade. Diante disso, um fantoma simples foi desenvolvido pela AIEA, utilizando materiais como cobre, acrílico e alumínio, para ser utilizado com o software Automated Tool for Image Analysis (ATIA), que realiza análises automáticas das imagens, extraindo dados do cabeçalho DICOM e exportando-os para um arquivo CSV para análise em planilhas Excel®. Os objetivos deste trabalho foram: (a) fabricar o fantoma de acordo com o modelo padrão da publicação IAEA Human Health Series No. 39; (b) aplicar o software ATIA no monitoramento diário de uma unidade de mamografia e do receptor de imagem digital (DR) adaptado a uma unidade de mamografia analógica no Laboratório de Radioproteção Aplicada à Mamografia (LARAM) do CDTN; (c) avaliar e comparar as respostas obtidas entre o software ATIA automatizado e o software IMAGEJ manual. Os resultados demonstraram a estabilidade e consistência do sistema de mamografia em métricas como SDNR e SNR, essenciais para garantir a qualidade da imagem. No entanto, variabilidades na MTF horizontal e vertical em frequências espaciais mais baixas indicam discrepâncias na resolução de detalhes finos. O índice de detectabilidade (D') destacou-se pela alta consistência, indicando a confiabilidade do sistema de mamografia na detecção de pequenos detalhes. Dessa forma, é possível inferir que diferenças significativas entre os softwares de controle de qualidade em várias métricas ressaltam a importância de uma seleção cuidadosa do software para atender às necessidades específicas de avaliação mamográfica.

Palavras-chave: Mamografia, Controle de qualidade, Automatização.

1. INTRODUCTION

Mammography is crucial for early detection of breast cancer, requiring periodic quality controls to ensure that images and patient exposure doses comply with regulatory limits. However, there are challenges in ensuring the efficiency and effectiveness of equipment, such as: negligence in mammography tests due to a lack of qualified personnel [1]; the fact that the only daily test recommended by national regulations involves a subjective evaluation using phantoms, which can lead to uncertainties; furthermore, the annual frequency of quantum efficiency tests is inadequate for detecting short-term fluctuations [2,3,4].

To ensure consistency in daily or weekly tests, it is crucial to incorporate automated and remote quality control tools. In this regard, the IAEA has developed a simple phantom with precise metrics, made of readily available materials (copper, acrylic, and aluminum), for mammography quality control. This phantom was designed to be used with the Automated Tool for Image Analysis (ATIA) software, also developed by the IAEA, which allows for automatic analysis of images, extraction of data from the Digital Imaging and Communications in Medicine (DICOM) header, export to a comma-separated values (.CSV) file, and finally, data reading by an Excel® spreadsheet, in a remote and automated manner [5,6].

The objectives of this work were: (a) to manufacture the phantom for mammography according to the standard mold recommended by the IAEA Human Health Series–No. 39 publication; (b) to apply the ATIA software in the daily monitoring of the mammography unit and the digital radiography (DR) image receptor retrofitted to an analog mammography unit at the Laboratory of Radioprotection Applied to Mammography (LARAM) of the Center for the Development of Nuclear Technology (CDTN); (c) to evaluate and compare the responses obtained between the automated ATIA software and the manual IMAGEJ software.

2. MATERIALS AND METHODS

2.1. Materials

The mammography phantom was manufactured, consisting of two parts: the first part includes four polymethylmethacrylate (PMMA) plates with uniform attenuation, each measuring 24 cm x 30 cm x 1 cm; the second part comprises a PMMA target plate with dimensions of 24 cm x 30 cm x 0.5 cm, containing a square piece of copper (Cu) measuring 5 x 5 cm and 1 mm in thickness, with edges finely filed with a needle file, and a piece of aluminum (Al) measuring 1 cm x 1 cm and 0.02 cm in thickness [5]. The manufactured phantom is shown in Figure 1.

Figure 1: Mammography phantom manufactured according to IAEA standards. The copper piece is located in the lower central region, and the aluminum piece is positioned in the upper right region.

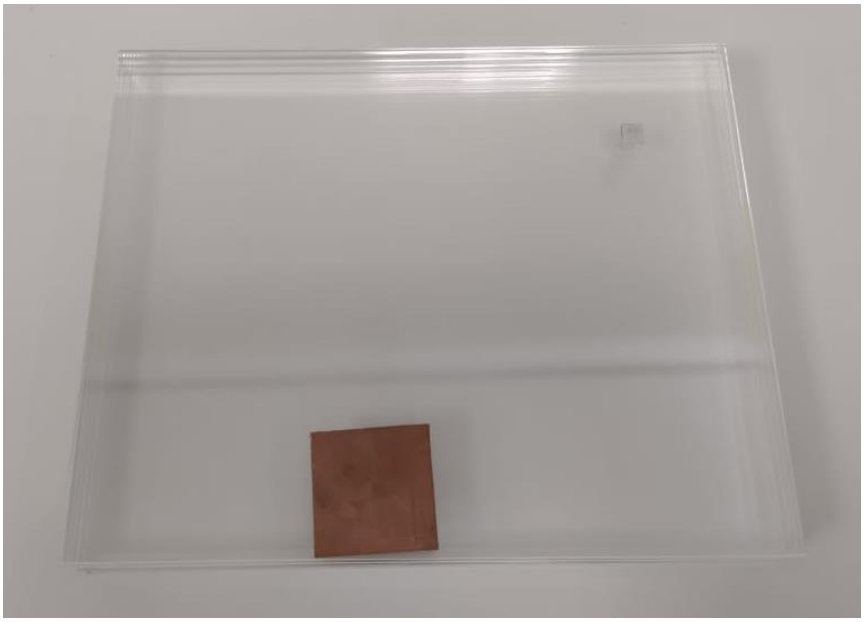

Source : Author's archives.

For image acquisition, a retrofit DR image detector, model RoseM (RSM 2430C) from Shimadzu, designed for digital X-ray images in breast diagnostics and compatible with general-purpose analog systems, was used, as shown in Figure 2 [7]. This detector was coupled with an analog mammography unit, model Mammomat 3000 Nova, from Siemens, as shown in Figure 3.

Figure 2: Retrofit image detector, model RoseM, manufacturer Shimadzu, size 24 cm x 30 cm for mammography.

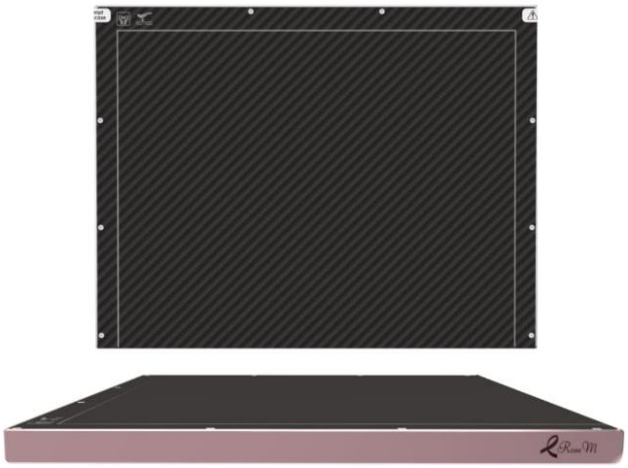

Source : DRTECH, 2017.

For automated image analysis, the IAEA Automated Tool for Image Analysis (ATIA) software was used. Furthermore, to compare the accuracy of the responses, the IMAGEJ [8,9] software was also used through a manual analysis methodology. The comparison was carried out using Minitab statistical software version 18 [10].

Figure 3: Siemens mammography unit, model Mammomat 3000 Nova, from LARAM.

Source : Author's archives.

2.2. Methods

According to the IAEA methodology, present in the Human Health Series–No. 39, images can be acquired daily or weekly. In this study, images were acquired daily for thirty days to monitor stability, maintaining specific exposure parameters for the Molybdenum-Molybdenum (MoMo) target-filter combination: 28 peak kilovolts (kVp) with 63 milliampere-seconds (mAs), which are considered standard parameters for quality control. Additionally, to compare response accuracy and variability, three images were acquired with the MoMo target-filter combination at three different parameters: 24 kVp and 40 mAs; 28 kVp and 63 mAs; and 32 kVp and 40 mAs.

The phantom was consistently positioned with the copper piece facing the thoracic edge of the bucky to ensure reproducibility of acquisition [5]. When importing images into the ATIA software, regions of interest (ROIs) are automatically positioned and can be manually adjusted, as shown in Figure 4.

Figure 4: ATIA software interface for the mammography phantom along with automatic ROIs.

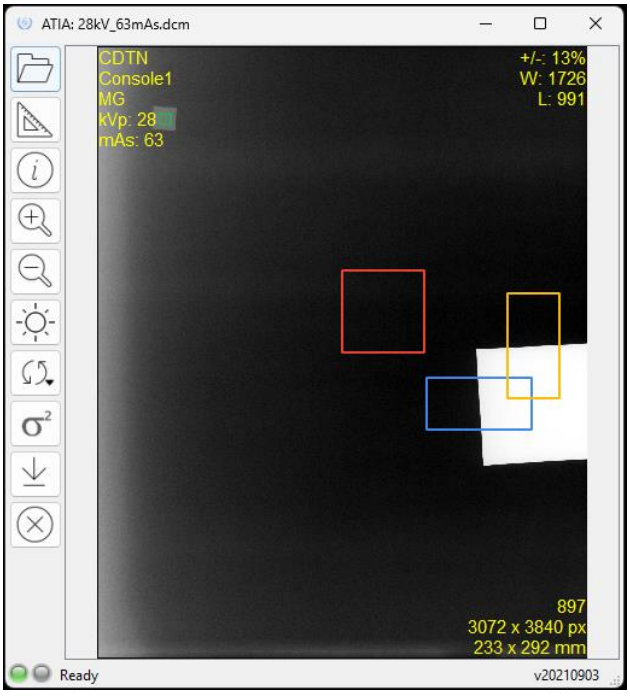

Source : Author's archives.

ROIs 1 and 2 measure Modulation Transfer Functions (MTFs) for horizontal and vertical edges, using Fourier transform on images with sharp edges. ROIs 3 and 4 are used to calculate the Signal-to-Noise Ratio (SNR) and Differential Signal-to-Noise Ratio (SDNR) according to equations (1) and (2), both present in the IAEA Human Health Series No. 39 [3], where PV is the average pixel value and SD is the standard deviation. The subscripts BG refer to background and Al to aluminum. The detectability index (d') is a mathematical model of an observer that depends on various image quality metrics, such as spatial frequency, MTF, contrast (C), visual transfer function (VTF), NNPS, and the Fourier transform of circular objects (S) with diameters of 0.1 and 0.25 mm for mammography, as shown in Equation 3, present in the IAEA Human Health Series No. 39 [5]. From the measurements taken, a CSV document was extracted from the ATIA software and analyzed using an Excel® spreadsheet, where graphs are generated for each metric.

$$SNR = \frac{PV_{BG}}{SD_{BG}} \tag{1}$$

$$SDNR = \frac{PV_{bg} - PV_{Al}}{SD_{bg}} \tag{2}$$

$$d' = \frac{\sqrt{2\pi C}\int_0^\infty S^2(u)\,MTF^2(u)\,VTF^2(u)\,udu}{\sqrt{\int_0^\infty S^2(u)\,MTF^2(u)\,VTF^4(u)\,NNPS(u)\,udu}} \tag{3}$$

For response comparison with IMAGEJ, the following metrics were considered: MTF, SNR, and SDNR. For the calculations, the images were inserted into IMAGEJ, and all processes were done manually, such as: inclusion of a 3.6 cm x 3.6 cm ROI in the background to obtain the average pixel value (PV) and standard deviation (SD) to measure SNR; addition of a 0.5 cm x 0.5 cm ROI in the aluminum to obtain the average pixel value (PV) and standard deviation (SD) to measure SDNR; and inclusion of images in the COQ plugin to measure the MTF.

All collected data were processed in Excel using the previously mentioned equations, and for comparison, the statistical software Minitab version 18 was used, where paired T-

tests were performed, considering a statistical significance of 5%. The null hypothesis considers that the difference between the population means is not equal to the hypothetical difference, and the alternative hypothesis considers that there is insufficient evidence to conclude that the mean difference between paired observations is statistically significant.

3. RESULTS AND DISCUSSIONS

3.1. Daily monitoring

For daily monitoring, the following metrics were considered: SDNR, SNR, MTF in both horizontal and vertical orientations, D' prime for different visible diameters in an image (0.1 mm and 0.25 mm), and the exposure index. Table 1 presents a summary of the data measured over 30 days of monitoring conducted on the Mammomat 3000 Nova mammography unit equipped with the retrofit plate.

Table 1 : Analysis of metric variability

	SDNR	SNR	MTF Hor. (ln/mm)			MTF Vert. (ln/mm)			D' prime		Exposure index
			50%	20%	10%	50%	20%	10%	D=0.1mm	D=0.25mm	
SD	0.51	2.16	0.29	0.71	0.98	0.29	0.52	0.94	0.02	0.11	37.84
Mean	5.13	23.52	2.04	4.02	5.33	2.03	3.00	5.11	1.23	7.32	164.00
CV (%)	10.01	9.18	14.14	17.77	18.43	14.06	17.33	18.29	1.44	1.46	23.07

SD = Standard deviation ; CV = Coefficient of variation.

Figure 5 (a) shows the SDNR and SNR metrics. The SDNR has a standard deviation of 0.51 and a mean of 5.13, resulting in a coefficient of variation of 10.01%. This indicates moderate variation over the 30 days of monitoring, suggesting reasonable consistency in the performance of the mammography equipment in terms of signal differentiation relative to noise. The SNR has a standard deviation of 2.16 and a mean of 23.52, with a coefficient of variation of 9.18%. This low coefficient of variation indicates that the mammograph has

quite consistent performance in terms of the signal-to-noise ratio, with relatively small variations over the monitored period.

The D' prime values, for both 0.1mm and 0.25mm, have very low coefficients of variation (1.44% and 1.46%, respectively). This indicates high consistency in the mammography equipment's ability to detect differences in small details over the 30 days, as shown in Figure 5 (b). This consistency in reproducibility is also present in the work by Mora *et al.* [1], where the coefficients of variation found are 1.4% for both diameters (considering phantom movement) and 1.5% and 1.6% for the diameters of 1 mm and 0.25 mm respectively (without phantom movement).

Figure 5: Tracking period of the mammography retrofit DR plate for (a) SDNR and SNR parameters, and (b) d' detectability index.

(a) (b)

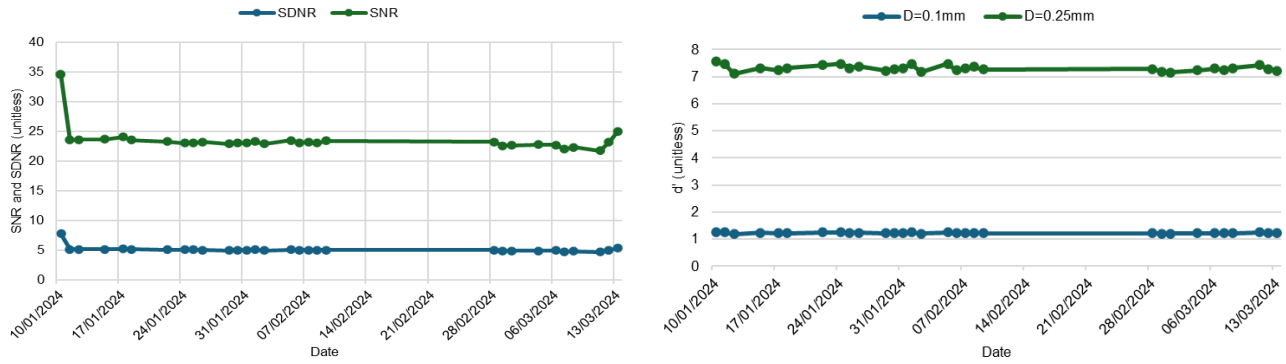

Source: Author's archives.

Figure 6 (a) shows that the Horizontal MTF exhibits greater variation as spatial frequency decreases (from 50% to 10%), with the coefficient of variation increasing from 14.14% to 18.43%. This indicates that the horizontal spatial resolution of the mammograph has increasing variability at lower spatial frequencies. The Vertical MTF, Figure 6 (b), follows a similar pattern to the Horizontal MTF, with the coefficient of variation increasing from 14.06% to 18.29% as spatial frequency decreases. This suggests that the variability in vertical spatial resolution also increases at lower spatial frequencies. These average MTF values,

presented in Table 1, were also similar to those found in the DR mammography equipment in the work by Fogagnoli *et al.* [9], where it was obtained: 2.339 (MTF Hor. 50%); 4.553 (MTF Hor. 20%); 6.151 (MTF Hor. 10%); 2.397 (MTF Vert. 50%); 4.566 (MTF Vert. 20%); and 6.115 (MTF Vert. 10%).

The exposure index has a standard deviation of 37.84 and a mean of 164.00, with a coefficient of variation of 23.07%. This is the highest coefficient of variation among all the metrics, indicating that exposure varies significantly over the monitored period, suggesting potential fluctuations in the dosimetry of the mammography equipment.

Figure 6: Tracking period of the mammography retrofit DR plate for (a) Horizontal MTF (50%, 20%, and 10%) and (b) Vertical MTF (50%, 20%, and 10%).

(a) (b)

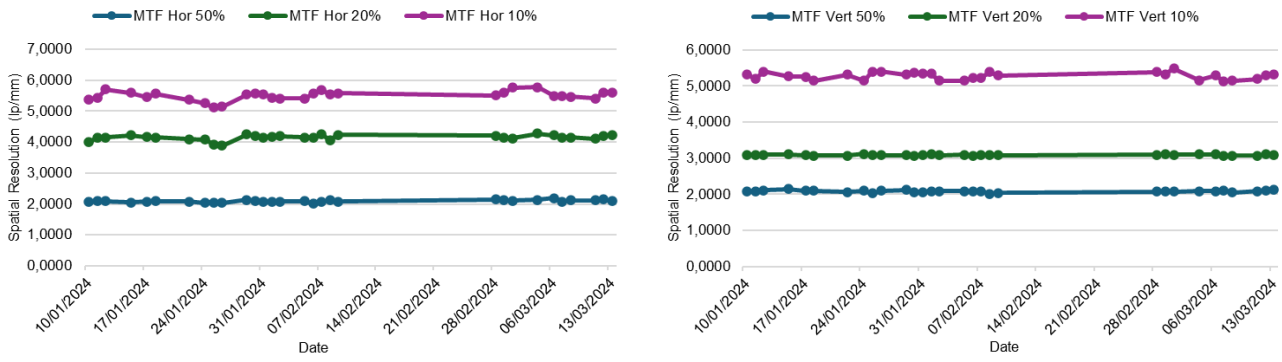

Source: Author's archives.

Figure 7 displays variance maps of three images representing three phases of monitoring: First day, intermediate day, and last day. A persistent artifact was observed in the lower region of the image and at the same position. A further study will be conducted to investigate the causes of this artifact. However, the image plate exhibits significant homogeneity across almost its entire extent.

Figure 7: Variance maps of the retrofit DR mammography plate collected in three different phases, being (a) from 10/01/2024, (b) from 01/02/2024, and (c) from 13/03/2024.

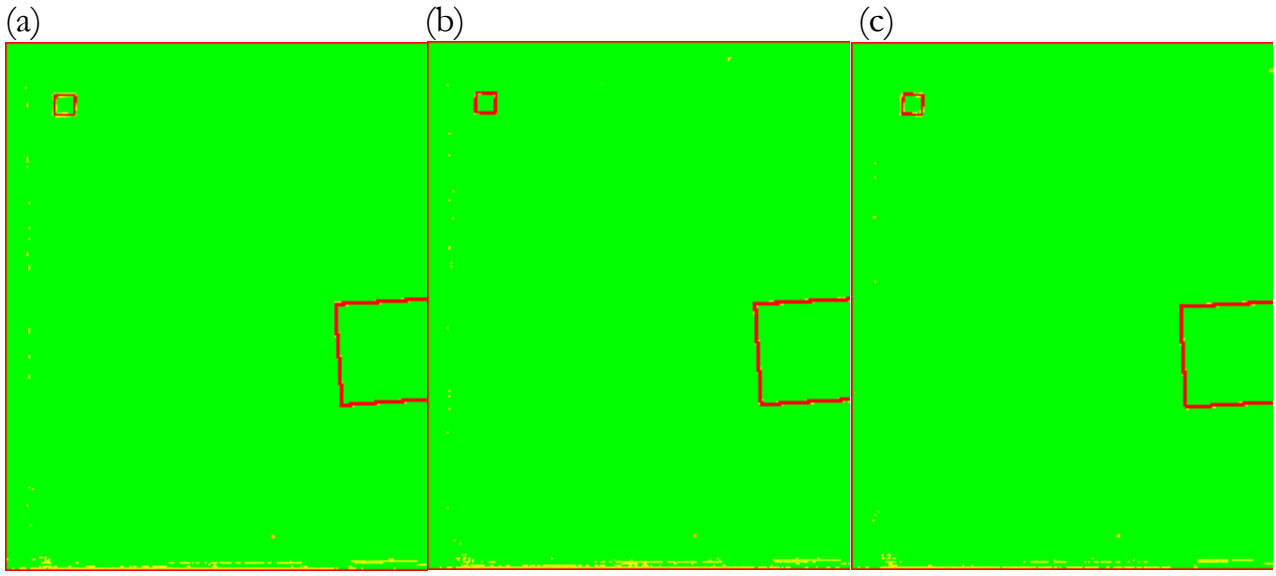

Source: Author's archives.

In addition to the consistency observed in the metrics evaluated throughout the daily monitoring, the practical feasibility of the remote use of the tool stands out. During the system application, different methods of digital image transfer for analysis were tested: physical media such as DVDs and USB drives, as well as digital methods such as cloud storage. All of these methods proved functional and did not compromise the automated analysis performed by the ATIA software. This enables the quality control professional in mammography to receive and evaluate images remotely, without the need to be physically present at the acquisition site, thus promoting the continuity and decentralization of the quality control process.

3.2. Comparative analysis

3.2.1. Estimated pairwise difference

Table 2 presents the paired difference estimate (mean and standard deviation) between the two quality control software packages for different Target-filter combinations.

Table 2: Paired t-test showing the paired difference estimate

Target-filter	SNR	SDNR	MTF 50% Hor.	MTF 20% Hor.	MTF 10% Hor.	MTF 50% Vert.	MTF 20% Vert.	MTF 10% Vert.
MoMo	-17.31 ± 5.76	-9.94 ± 3.49	-0.26 ± 0.03	-1.18 ± 0.67	1.15 ± 1.20	0.01 ± 0.19	-1.45 ± 0.37	-0.23 ± 0.40
MoRh	-19.01 ± 6.35	-11.23 ± 3,17	-0.20 ± 0.09	-0.67 ± 0.34	0.21 ± 1.54	-0.01 ± 0.04	-1.33 ± 0.28	-0.34 ± 0.43
WRh	-20.24 ± 4.67	-11.42 ± 2.83	-0.20 ± 0.04	-0.48 ± 0.51	-0.83 ± 0.06	-0.10 ± 0.02	-1.37 ± 0.27	-0.66 ± 0.14

The analysis of Signal-to-Noise Ratio (SNR) revealed that the SNR difference is negative for all target/filter combinations: MoMo (-17.31 ± 5.76), MoRh (-19.01 ± 6.35), and WRh (-20.24 ± 4.67), while the relatively high standard deviation suggests significant variation in the results. Similarly, the difference in SDNR is also negative for all combinations: MoMo (-9.94 ± 3.49), MoRh (-11.23 ± 3.17), and WRh (-11.42 ± 2.83). This indicates that the performance of the software in SDNR consistently differs among the target/filter combinations, with variations that should be taken into consideration.

For Horizontal MTF 50%, the differences are negative and quite consistent: MoMo (-0.26 ± 0.03), MoRh (-0.20 ± 0.09), and WRh (-0.20 ± 0.04). These results indicate a relatively minor and stable difference between the software packages for this metric, suggesting comparability in terms of Horizontal MTF 50%. Regarding Horizontal MTF 20%, we observe greater variation, especially for MoMo (-1.18 ± 0.67), compared to MoRh (-0.67 ± 0.34) and WRh (-0.48 ± 0.51). These results indicate that the difference between the software packages is more pronounced and variable, particularly for MoMo. Analysis of Horizontal MTF 10% shows that MoMo has a positive difference (1.15 ± 1.20), whereas MoRh (0.21 ± 1.54) and WRh (-0.83 ± 0.06) show negative differences. WRh exhibits a more stable difference with a smaller standard deviation, highlighting consistency.

For Vertical MTF 50%, the differences are close to zero, especially for MoMo (0.01 ± 0.19) and MoRh (-0.01 ± 0.04), indicating little difference between the software packages

for this metric. WRh (-0.10 ± 0.02) shows a slightly larger difference, but still small. The differences in Vertical MTF 20% are negative and consistent: MoMo (-1.45 ± 0.37), MoRh (-1.33 ± 0.28), and WRh (-1.37 ± 0.27). With little variation, these results suggest comparable differences between the software packages for this metric. Finally, in Vertical MTF 10%, WRh shows a larger and more consistent difference (-0.66 ± 0.14) compared to MoMo (-0.23 ± 0.40) and MoRh (-0.34 ± 0.43), which exhibit larger variations. This underscores the stability of WRh in terms of Vertical MTF 10%.

3.2.2. P-Value

Table 3 displays the "p" values for the 5% significance level for different Target-Filter combinations.

Table 3: P-Value test for the 5% significance level

Target-filter	SNR	SDNR	MTF 50% Hor.	MTF 20% Hor.	MTF 10% Hor.	MTF 50% Vert.	MTF 20% Vert.	MTF 10% Vert.
MoMo	0.04	0.04	0.01	0.09	0.24	0.95	0.02	0.43
MoRh	0.04	0.03	0.06	0.08	0.83	0.70	0.01	0.31
WRh	0.02	0.02	0.02	0.24	0.00	0.02	0.01	0.01

For MoMo, both SNR and SDNR have a "p" value of 0.04. In the case of MoRh, SNR has a "p" value of 0.04 and SDNR of 0.03. For WRh, both SNR and SDNR have a "p" value of 0.02. These relatively low "p" values indicate that there is a statistically significant difference in SNR and SDNR results between the two quality control software packages, suggesting a significant performance difference.

For Horizontal MTF 50%, MoMo has a "p" value of 0.01, indicating a significant difference. MoRh, with a "p" value of 0.06, does not show a significant difference, while WRh, with a "p" value of 0.02, also shows a significant difference. This suggests that for this metric, MoMo and WRh have significantly different performances between the software packages, while MoRh does not. None of the Target-filter combinations show significant "p" values for Horizontal MTF 20%. MoMo has a "p" value of 0.09, MoRh of 0.08, and

WRh of 0.24, all indicating that there are no statistically significant differences between the software packages for this metric. For Horizontal MTF 10%, only WRh has a significant "p" value (0.00), indicating a significant difference between the software packages. MoMo and MoRh have "p" values of 0.24 and 0.83, respectively, suggesting no significant difference for these Target-filters.

Regarding Vertical MTF 50%, only WRh has a significant "p" value (0.02). MoMo and MoRh, with "p" values of 0.95 and 0.70 respectively, do not show significant differences between the software packages for this metric. All Target-filter combinations show significant "p" values for Vertical MTF 20%: MoMo with 0.02, MoRh with 0.01, and WRh also with 0.01. This indicates a significant difference in software performance for this metric across all combinations. For Vertical MTF 10%, only WRh has a significant "p" value (0.01), indicating a significant difference between the software packages. MoMo and MoRh, with "p" values of 0.43 and 0.31, respectively, do not show significant differences for this metric.

4. CONCLUSIONS

The phantom used is easy to fabricate and cost-effective. The ATIA software provides a simple interface, performs automated calculations, and stores results in spreadsheets, which are available free of charge and compatible with those provided by the IAEA for metric tracking. Metrics such as SDNR and SNR demonstrated stable and consistent operation of the mammography system, essential for ensuring image quality. However, analyses of Horizontal and Vertical MTF revealed greater variability at lower spatial frequencies, indicating challenges in resolving fine details. The D' prime metric stood out for its high consistency, indicating the mammography system's reliability in detecting small details, despite observed variability in exposure index, underscoring the need for rigorous dosimetry control to ensure safety and image accuracy.

Regarding the remote application, various methods of image transfer were tested — including physical media such as DVDs and USB drives, as well as digital methods like cloud services and PACS — and all were successful. This demonstrates that quality control can be performed remotely, enabling continuous and efficient monitoring by the responsible professionals, regardless of the physical location of the equipment.

Furthermore, differences noted between quality control software for various metrics and target-filter combinations underscore the importance of careful software selection tailored to specific mammographic evaluation needs. Significant variations in SNR, SDNR, and MTF among software options emphasize the necessity of considering these differences when choosing the most suitable system for clinical environments. Despite potential result variations, ongoing monitoring of system performance over time remains feasible and crucial for maintaining consistency and quality in mammography procedures.

ACKNOWLEDGMENT

This work was supported by the Brazilian National Council for Scientific and Technological Development (CNPq, INCT/INAIS Project – 406303/2022-3 and CNPq Process 308368/2022-3 – Productivity Fellowship and Master's Scholarship), the Minas Gerais State Research Support Foundation (FAPEMIG), and the Nuclear Technology Development Center (CDTN).

CONFLICT OF INTEREST

The authors of this article declare that there are no conflicts of interest, financial or otherwise, that could have influenced the results or conclusions presented. All data and

analyses were conducted objectively, aiming to contribute to the advancement of scientific knowledge in the relevant field.

REFERENCES

[1] MORA, P. ; PFEIFFER, D. ; ZHANG, G. *et al.* The IAEA remote and automated quality control methodology for radiography and mammography. **Journal of Applied Clinical Medical Physics**, Louisville, vol 22, p. 1–17, 2021.

[2] BRAZIL. Ministério da Saúde. Diretoria Colegiada da Agência Nacional de Vigilância Sanitária. Instrução Normativa IN Nº 92, de 27 de maio de 2021. Brasília, DF: **Diário Oficial da União**, 2021.

[3] BRAZIL. Ministério da Saúde. Diretoria Colegiada da Agência Nacional de Vigilância Sanitária. RDC Nº 611, de 9 de março de 2022. Brasília, DF: **Diário Oficial da União**, 2022.

[4] EFOMP - European Federation of Organizations for Medical Physics. EFOMP Mammo Protocol. Quality controls in Digital Mammography. 2017.

[5] IAEA - International Atomic Energy Agency. Implementation of a Remote and Automated Quality Control Programme for Radiography and Mammography Equipment. Vienna: Human Health Series nº39. Disponível em: https://www.iaea.org/publications/13539/implementation-of-a-remote-and-automated-quality-control-programme-for-radiography-and-mammography-equipment. Acesso em: 17 jun. 2024.

[6] IAEA - International Atomic Energy Agency. Remote/Automated quality control in Radiology. Vienna: Human Health Series nº39. Disponível em: https://humanhealth.iaea.org/HHW/MedicalPhysics/DiagnosticRadiology/PerformanceTesting/AutomatedQAinRadiology/index.html. Acesso em: 17 jun. 2024.

[7] DRTECH Co, Ltd. "RSM1824C / RSM2430C User Manual". Disponível em: https://www.drtech.co.kr/kr/. Acesso em: 01 jun. 2024.

[8] DONINI, B. *et al.* Free software for performing physical analysis of systems for digital radiography and mammography. **Medical physics**, Bolonha, v. 41, n. 5, p. 051903, 2014.

[9] FOGAGNOLI, M. P. *et al.* Implementação de um Programa de Controle de Qualidade Remoto para Avaliação de Imagens em Radiografia Convencional e Mamografia. **Revista Brasileira de Física Médica**, São Paulo, v. 16, p. 696-696, 2022.

[10] MINITAB. Minitab Statistical Software, versão 18 [software]. State College, PA: Minitab, Inc., 2017.

LICENSE